It Used To Be Dark Here: Geolocation Calibration of the Defense Meteorological Satellite Program Operational Linescan System

One Sentence Description

A repeatable process for a geolocation accuracy assessment of the Defense Meteorological Satellite Program Operational Linescan System using an active calibration target is presented and geolocation accuracy of the current constellation is reported.

List of Authors

Benjamin T. Tuttle; University of Denver, Department of Geography; 328 W. Elm St., Louisville, CO 80027; benjamin.tuttle@gmail.com

Sharolyn J. Anderson; School of Natural & Built Environments & Barbara Hardy Institute; University of South Australia; University of South Australia, Mawson Lakes Campus Adelaide SA 5095; Sharolyn.Anderson@unisa.edu.au

Paul Sutton; Barbara Hardy Institute and School of Natural and Built Environments, University of South Australia, Adelaide, South Australia, Australia 5001;& University of Denver, Department of Geography; psutton@du.edu

Christopher D. Elvidge; National Geophysical Data Center; 325 Broadway, E/GC2, Boulder, CO 80305; chris.elvidge@noaa.gov

Kim Baugh; University of Colorado, Boulder, Cooperative Institute for Research in Environmental Science; 325 Broadway, E/GC2, Boulder, CO 80305; kim.baugh@noaa.gov

Abstract

Nighttime satellite imagery from the Defense Meteorological Satellite Program (DMSP) Operational Linescan System (OLS) has a unique capability to observe nocturnal light emissions from sources including cities, wild fires, and gas flares. Data from the DMSP OLS is used in a wide range of studies including mapping urban areas, estimating informal economies, and estimations of population. Given the extensive and increasing list of applications a repeatable method for assessing geolocation accuracy would be beneficial. An array of portable lights was designed and taken to multiple field sites known to have no other light sources. The lights were operated during nighttime overpasses by the DMSP OLS and observed in the imagery. An assessment of the geolocation accuracy was performed by measuring the distance between the GPS measured location of the lights and the observed location in the imagery. A systematic shift was observed and the mean distance was measured at 2.9km.

INTRODUCTION

Images of the Earth at night have become a spatially explicit global icon depicting human presence and activity on the surface of planet earth. These images are unequivocally a striking measure of the world's urban population. Nighttime lights data have been used to estimate urban populations and intra-urban population density (Sutton *et al.* 1997; Sutton 1997; Sutton *et al.* 2003). Not surprisingly, nighttime lights have also been demonstrated to be a reasonable proxy measure of energy consumption at national and sub-national scales (Elvidge *et al.,* 1997b; Lo, 2001). In addition, the images of the Earth at night have been used to map urban and exurban areas (Cova *et al.*, 2004; Imhoff *et al.,* 1997; Henderson *et al.,* 2003; Schneider *et al.*, 2003; Small *et al.,* 2005).

Much of nocturnal lighting is not due to city lights and is associated with forest fires. Data products derived from time series analysis of the nightly observations of the earth have been used to estimate forest area impacted by wildfires (Elvidge *et al.*, 2001b), and inform studies of net primary productivity and carbon modeling (Milesi *et al.*, 2003). Models have been developed to produce digital maps of percent pavement (i.e. impervious surface area) by using nighttime satellite imagery in conjunction with global representations of the variation of human population density (Elvidge *et al.* 2004a, 2007). Nocturnal satellite observations not only observe forest fires but also make direct observations of gas flaring (the burning off of low molecular weight hydrocarbons such as methane, ethane and propane) in areas of the world where oil is being drilled and refined. Models have been developed from these observations to monitor global gas flaring volumes (Elvidge *et al.*, 2009). There is increasing interest in utilizing nocturnal observations of the Earth to make independent estimates of economic activity for

disaggregated spatial units and for mapping and estimating informal economies in parts of the world where good economic data is difficult to obtain (Ghosh *et al.,* 2009, 2010). Digital observations of the Earth at night have been obtained by several satellite platforms and from the International Space Station; however, most of these systematic studies utilizing Earth at night imagery are drawn from data products derived from satellite images of the Defense Meteorological Satellite Program's Operational Linescan System (DMSP OLS).

Nighttime satellite imagery is distinct, as it observes emitted rather than reflected radiation. Data products derived from DMSP OLS nighttime satellite imagery are used for an increasing number of applications. The coarse spatial resolution of the DMSP OLS imagery presents some interesting challenges with respect to characterizing the positional accuracy of the images. This paper presents a methodology for characterizing the geo-location accuracy of the standard geo-referenced image products provided by the National Geophysical Data Center (NGDC). In short, we travelled to "dark" places and lit them up with a portable light source that was detected by the DMSP OLS. We compared GPS coordinates taken at these "dark" sites to the location of the "new" light detected by the DMSP OLS.

The DMSP OLS was first launched in 1972. Each satellite is in a sun-synchronous near-polar orbit of 104 minutes at an altitude of 830km above the Earth's surface. The sensor has a 3000km swath and provides global coverage two times per day. The DMSP satellites are flown in either a dawn-dusk or day-night orbit. The OLS has a thermal band which is sensitive to radiation from 10.0 – 13.4 um and a visible band sensitive to radiation from 0.58 – 0.91 um.

The DMSP OLS was designed to observe clouds; however, the use of the OLS's photo-multiplier tube (PMT) at night give the OLS a unique capability. During periods of low lunar illuminance and low cloud cover the OLS is able to observe nocturnal light emissions from the surface of the earth. This includes light emitted by cities, fires, gas flares, and heavily lit fishing boats, providing a way to observe the extent of human influence in ways that were not previously available on any other remote sensing platform.

The OLS collects data at a spatial resolution of $0.55km^2$ ground-sample distance (GSD) known as fine resolution. However, these data are converted to smooth resolution of $2.7km^2$ GSD by averaging a 5x5 grid of fine pixels for global coverage. A limited amount of higher resolution (fine) data is recorded and transmitted to the ground station based on requirements set by Air Force Weather Agency (AFWA). The instantaneous field of view (IFOV) of the fine resolution data, collected by the PMT, is $2.2km^2$ at nadir and expands to $4.3km^2$ at 800km from nadir. At 800km the PMT electron beam shifts to constrain the enlargement of pixels reducing the IFOV to $3km^2$. At the edge of the swath (1500km from nadir) the IFOV is $5.4km^2$. So the IFOV is significantly larger than the GSD. For the smooth resolution PMT data the IFOV at nadir is $5km^2$ and at the edge of the swath is approximately $7km^2$. More details on the OLS can be found at the NGDC website (http://www.ngdc.noaaa.gov/dmsp) and in publications by Elvidge *et al.* (2001a, 2004) and Baugh *et al.* (2010).

In 1992 the NGDC in Boulder, CO began a digital archive of the DMSP OLS data, prior to that the data were stored on film reels. NGDC provides the data in several forms ranging from raw orbits to geolocated annual composites. The annual composites

are made by collecting all the cloud-free data from the dark portion of the lunar cycle, thus avoiding the inclusion of moonlit clouds (Elvidge *et al.,* 1997a, 1999, 2001). These products have been found to overestimate the size of the lights on the ground (Small *et al.,* 2005). Despite this shortcoming the nighttime lights data collected by the OLS have been used in a wide variety of studies.

Assessment of positional accuracy is essential to understanding satellite imagery and improving the results of research relying on that imagery (Cuartero *et al.,* 2010; Dollof & Settergren 2010; O'Hara *et al.,* 2010; Qiao *et al.,* 2010; Surazakov & Aizen 2010). Given the breadth of applications a firmer understanding of the positional accuracy of the OLS is in order. Elvidge *et al.* (2004b) examined the positional accuracy of the OLS. This study examined the characteristics of the OLS on board satellites F10, F12, F14, and F15. The OLS data were compared to locations of point sources of light extracted from Landsat ETM+ 15m panchromatic data. The smooth data were found to have accuracies between 1.55 and 2.36km (less then the GSD of one smooth pixel) with satellite F14 having the best accuracy and satellite F10 the worst.

At present the two satellites flying in a day/night orbit (making them useful for the observation of nighttime lights) are F16 and F18. Neither of these satellites were in orbit at the time of the previous study. Additionally, rather than using Landsat data to extract locations, we have devised a new methodology. Our research has found that it is possible to construct a portable light source capable of detection by the OLS. We present the details of this light source as well as methods for determining the positional accuracy of the OLS using such a light source.

METHODS

Light Design

We set out with a need to design a portable light source that could be detected by the DMSP OLS. There are a wide variety of commercial lighting products available to choose from and some empirical studies were required to settle on an appropriate design. Many factors had to be considered including lumens/watts ratio, the spectral characteristics of the light source, and the ability to easily transport of the light source from one sight to another.

The field experiments were started using standard off the shelf halogen work lights (available at common chain hardware stores). Several field experiments proved that the halogen work lights were not bright enough to be detected by the OLS in quantities that could be easily powered in the field. In order to power enough of these lights to achieve detection would have required more power than could be easily transported. This is due to the halogen work light's low lumens/watts ratio.

This was followed by evaluating concentrated three million candle power hand held spotlights. Unlike the previously mentioned light sources measured in lumens these spot lights were measured in candle power. Lumens are a measure of the total visible light emitted by a source, while candle power (or candela) is a measure of the total visible light emitted by a source in a particular direction. These spotlights are designed to focus a beam of light on a specific location, hence the term spot light. The lights previously, mentioned and the lights eventually chosen for this study are omni-directional and their brightness is measured in lumens. The hand held spotlights are believed to have been bright enough if pointed directly at the sensor, but even with accurate predictions of the

sensor overpass it proved to be difficult to document proper or improper aiming on any given night.

This led to evaluating high intensity discharge (HID) lighting options. The current configuration relies on high pressure sodium lamps common in applications such as warehouse lighting. These lamps are available in varying sizes including 250 watts and 1000 watts, both used in these experiments.

These high pressure sodium lamps emit most of their energy in the orange to red portion of the visible spectrum from 560 – 740 um (figure 1). The emitted energy fits well within the optical window of the atmosphere. Additionally, these wavelengths are less prone to Rayleigh scattering than the shorter wavelengths produced by other high intensity discharge lighting options such as metal halide lamps. In addition high pressure sodium lamps have a higher ratio of lumens/watts than metal halide lamps. Also, the peak emissions from the high pressure sodium lamps are within the peak response of the OLS sensor's spectral response curve (figure 2). Elvidge *et al.* (2010) describe the spectral signatures of a variety of lighting types (including high pressure sodium) in an effort to document the optimal spectral bands to identify different lighting types.

The high pressure sodium lights were easily purchased from vendors online. The 1000 watt lamps emit approximately 140,000 lumens and the 250 watt lamps emit approximately 35,000 lumens. For reference, the average 100 watt incandescent lamp emits approximately 1500 lumens. Once the lights were purchased wooden frames were designed and built to hold the light pointing upwards as they are designed to hang from a ceiling and point down. The frames hold the capacitor, igniter, ballast, and socket for each lamp and are open on top to allow for the attachment of a 22-inch (55.88cm)

aluminum reflector and the lamps (figure 3). A total of eight 1000 watt high pressure sodium lamps and six 250 watt high pressure sodium lamps, the necessary frames for housing the fixture, and two 6000 watt gas generators fit on a 6-foot x 10-foot (1.83m x 3.05m) utility trailer (figure 4). Each 6000 watt generator can power up to four 1000 watt lamps at a time. This allowed for as many as eight 1000 watt lamps (approximately 1,120,000 lumens) or as little as one 250 watt lamp (approximately 35,000 lumens) at a time.

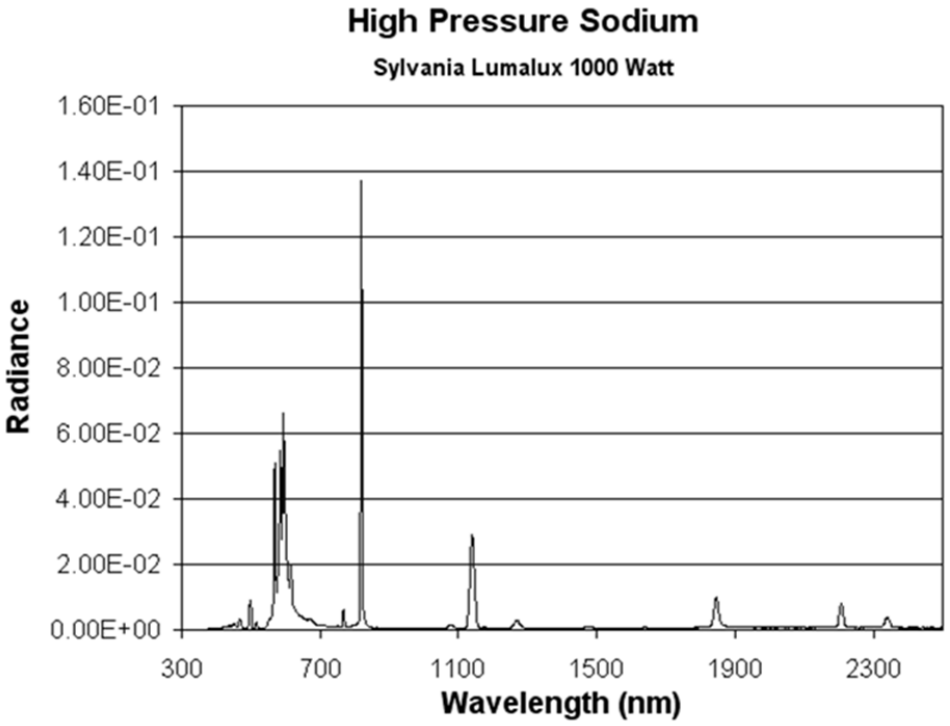

Figure 1-A high pressure sodium light bulbs spectral signature measured by an ASD spectrometer.

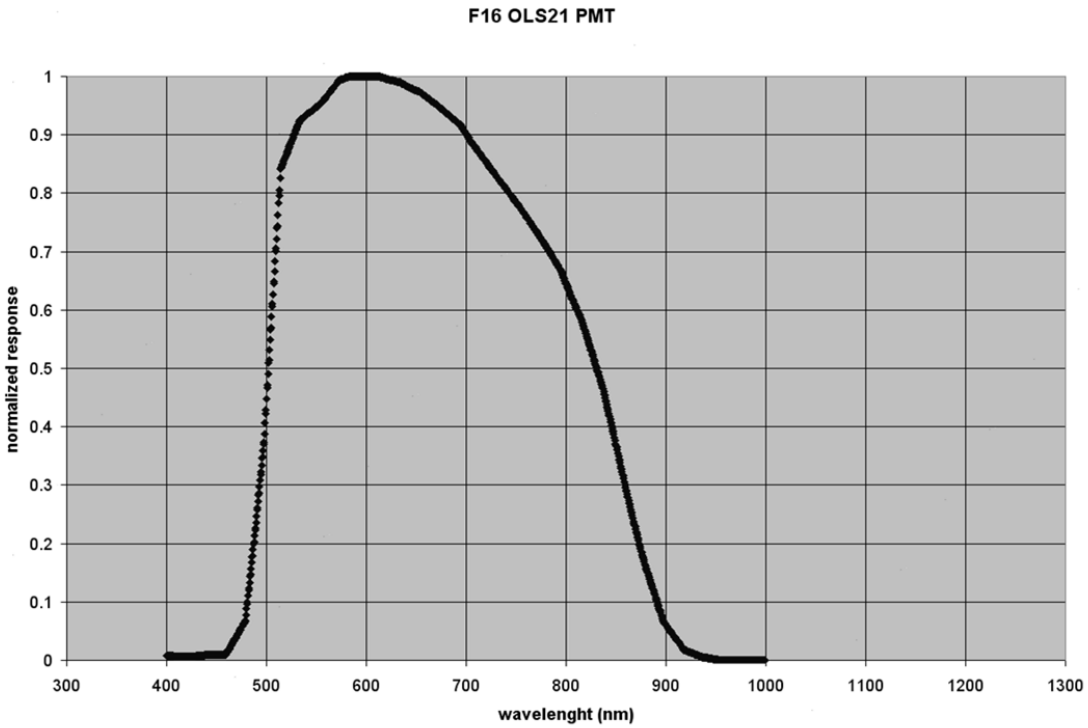

Figure 2 – The spectral response of the DMSP OLS from satellite F16, measured pre-flight.

Figure 3 – A 1000 watt high pressure sodium light with the aluminum reflector.

Figure 4 – Seven (1000 watt) high pressure sodium lights in the utility trailer and the two generators used to power the lights in the field.

Site Selection

Selecting the sites for these experiments involved several important factors. The requirements included accessibility, permission from land owners/managers, no other light sources or light pollution from nearby light sources, and accessibility to a truck and trailer throughout the year. Finding suitable locations that met all of these requirements was difficult. The identified sites that met the requirements range from approximately two to seven hours drive from the storage location of the lights.

One of the key factors in site selection was permission from the land managers of each location. Conducting the experiments at all sites were cleared with the relevant

parties and local authorities were notified of every experiment prior to our arrival. This was important, especially because the lights were visible from roads up to five miles away and have an orange glow similar to that of a wild fire. Despite these efforts there were still occasions when concerned passers by visited the site during an experiment to see why a light had appeared where there normally wasn't one.

All sites were required to be completely dark, meaning no other light sources in the vicinity or light pollution from neighboring light sources. Each site was visited and GPS coordinates were gathered and differentially corrected. These points were overlaid on DMSP OLS annual composites to determine if the site was completely dark. Only sites with a DN value of zero in the annual composites were considered. Additionally, the sites had to be accessible. The lights and required power were transported in a utility trailer. Each site needed to be accessible to a truck pulling the trailer.

The DMSP orbit prohibits the collection of data with a clear view of sites in our area of interest during the summer (approximately mid-May to early September) because the sun sets too late. This meant that we conducted these field experiments in the winter and weather was an important factor in site selection. A site that was covered in more than one foot of snow for most of the winter was not considered accessible. Additionally, sites with consistent and predictable weather were considered more desirable than those with unpredictable weather, given that clouds can obscure the view of the portable light and make the data unusable. A site near the peak of Mt. Evans was examined on several occasions and was very desirable as it was close to the location the lights were stored, on property controlled by the University of Denver, and dark. However, it was found that predicting the weather there was too difficult to be worth while. For example, on one

night with a prediction of clear skies it started snowing 30 minutes before the satellite was to make an observation of the site. On the other hands sites such as the Santa Fe National Forest proved to be very stable based on weather predictions allowing for a higher percentage of the visits there to yield usable data.

Multiple sites were chosen to control for systematic versus non-systematic shifts in the geolocation. Based on the criteria a total of three sites were chosen, two in Colorado and one in New Mexico. The sites were the Pawnee National Grasslands in northeast Colorado, the Karval State Wildlife Area in southeast Colorado, and the Santa Fe National Forest in Rowe, New Mexico (figure 5). Each of these sites met all the criteria determined for a suitable site and were visited on multiple occasions. The lighting caused by this equipment is clear in the DMSP OLS images taken on days ‘Before’, ‘During’ and ‘After’ the operation of the lights (figure 6).

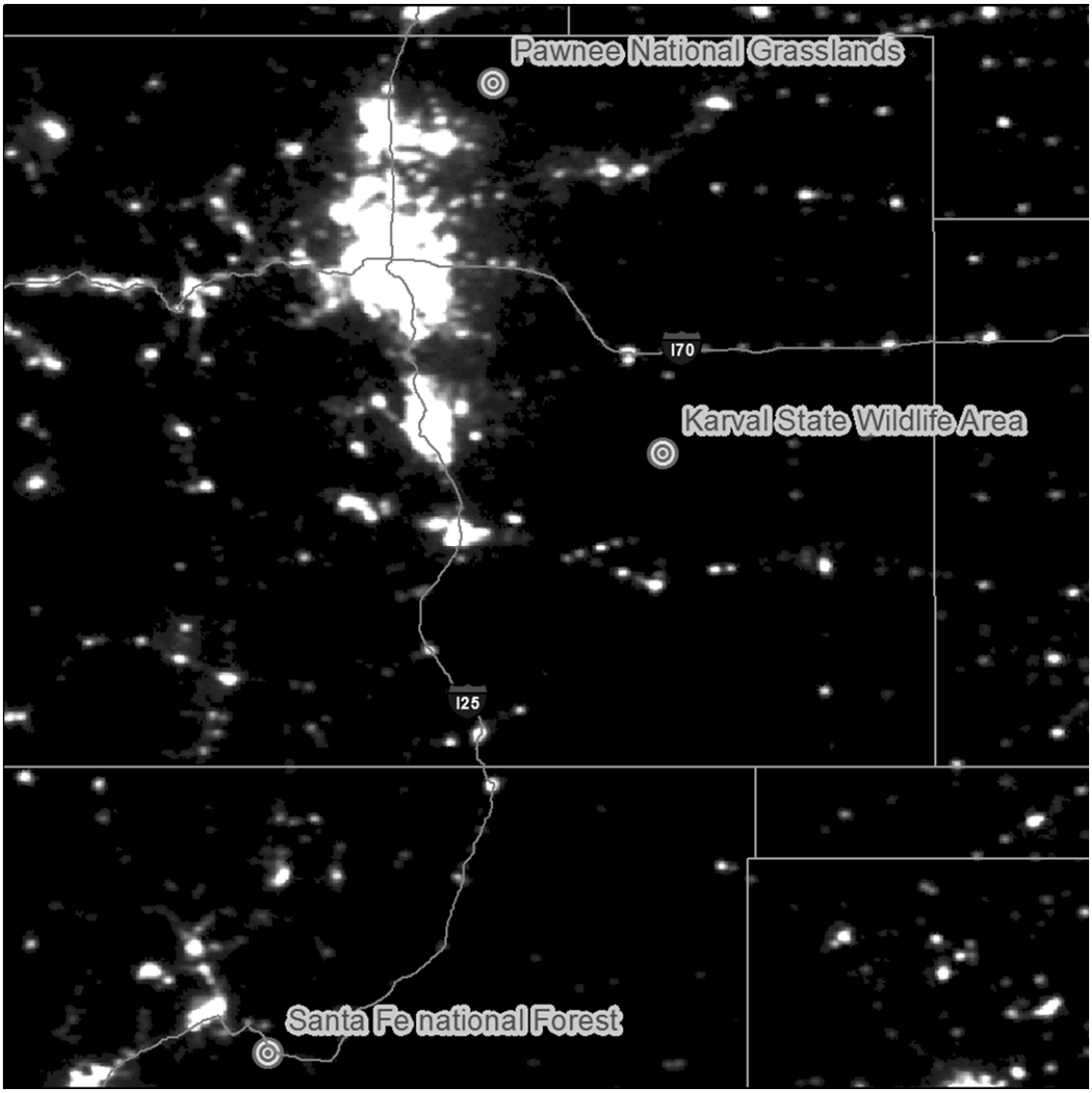

Figure 5 – Map of the three field sites in Colorado and New Mexico with a nighttime lights annual composite from satellite F16 for the year 2009 as the background.

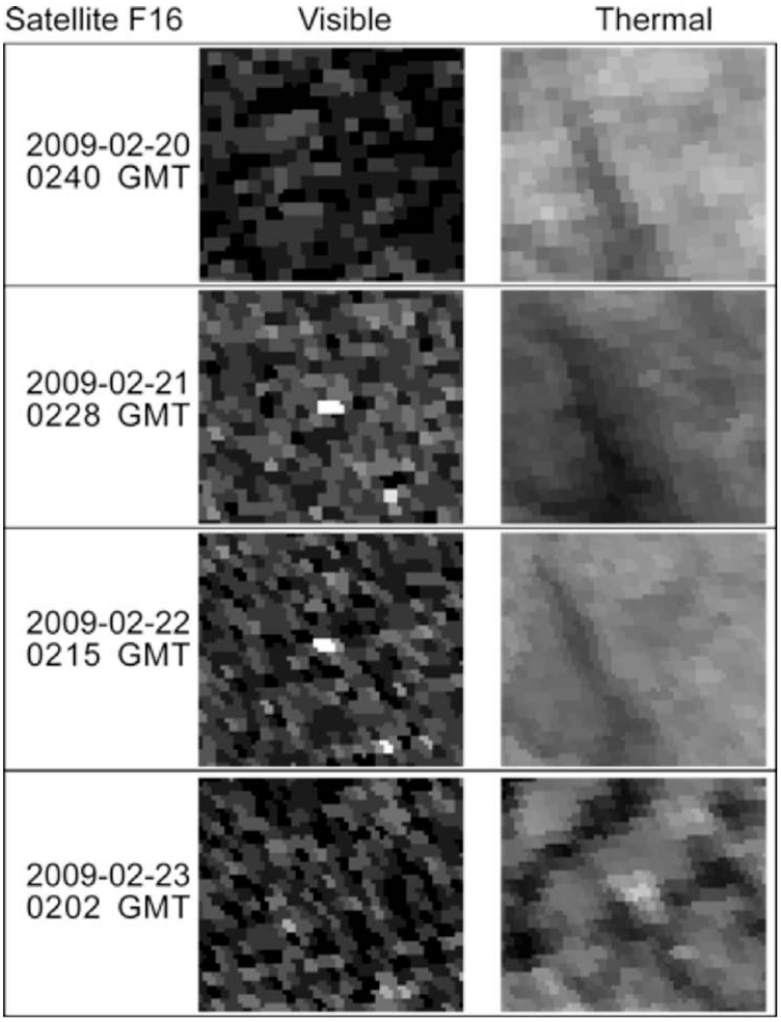

Figure 6 – DMSP OLS Images of the Karval site on four consecutive days with Lights in use on the two middle days (2009-02-21 & 2009-02-22).

Field Experiments

Using the ephemeris available to the NGDC for the DMSP the time of observation at each site was predicted for each season (September to May) along with other relevant details such as scan angle, lunar illuminance, and solar elevation. To avoid sun light or moon light in the imagery only nights when the solar elevation was less than 12 degrees and lunar illuminance was less than 0.0005 lux were considered for inclusion in the study. Using this information nights when the lunar illuminance and solar elevation

were within acceptable ranges for clear observations could be determined. Predictions of the observation time at each site were then calculated out in four week intervals as time went by to get more accurate times. In the experiments, the predicted time of observation was always within seconds of the actual time of observation. Following this the weather predictions at each site were monitored for times when there was a prediction of clear skies and the lunar illuminance and solar elevation were within acceptable ranges. Based on this information the nights to conduct the experiments were chosen.

When conducting the experiments the lights were set up well in advance of the predicted observation time. The trailer was always placed in the same location that the GPS coordinates were measured for each site. High pressure sodium lamps do not achieve their peak intensity when first turned on. To ensure that the lights achieved their peak brightness they were turned on 45 – 60 minutes prior to the predicted observation time. The lights were then left on until after the predicted observation times had passed. Different numbers of lights were used on different nights in order to be able to examine changes in observed brightness for use in other studies.

The possibility that pointing the lights at the sensor would achieve better results was considered. It is possible to calculate the direction and angle at which the sensor would observe the site on each night. However, our initial tests showed that with these lights there was no significant difference between pointing the light at the sensor and just pointing it straight up into the sky. This is likely because the 22 inch aluminum reflector, although it helps direct the light upwards, does not have enough of a concentrating effect to achieve any difference from pointing directly at the OLS sensor.

The OLS sensor typically observes a light source in more than one pixel as the ground footprint of the pixels overlap. These characteristics are further described by Elvidge *et al.* (2004) and the portable light source was observed in multiple pixels in the imagery on any given night. After returning to the lab this fact was clearly observed in the imagery of the portable light source. In the fine imagery the lights often registered in upwards of 10 pixels and in the smooth imagery commonly registered in 4 – 8 pixels, depending on the number of lights used on a given night.

There is never a single pixel that represents the light in the imagery collected; thus on each successful observation all the pixels in which the light source were detected were outlined in the imagery. The resulting polygon shapefile represented all the pixels in which the light was observed on each night. In order to identify a single latitude and longitude representing the location of the light in the imagery the centroid of each polygon was calculated using the "Feature to Point" tool in ArcGIS. The distance and bearing from the GPS latitude and longitude for the site to the observed latitude and longitude from the imagery was calculated using the Spherical Law of Cosines. The following equation for Spherical Law of Cosines distance was used:

```
Distance = ACOS(SIN(lat1)*SIN(lat2)+COS(lat1)*COS(lat2)*COS(lon2-lon1))*6371
```

(1)

In addition to the distance from the GPS point, the bearing from the GPS point to the observed location was calculated using the following equation:

```
Bearing = ATAN2(COS(lat1)*SIN(lat2)-SIN(lat1)*COS(lat2)*COS(lon2-lon1),
                SIN(lon2-lon1)*COS(lat2))
```

(2)

RESULTS and DISCUSSION

The results are reported in tables 1- 4 and show the mean, standard deviation, confidence interval, first quartile, median, and third quartile of the distance in kilometers and of the bearing in degrees (reported between -180° and 180° where north is 0°). The results are reported for all data points, separated by satellite, resolution, both satellite and resolution, and by field site. The overall statistics are based on 28 points. The geographic spread for the points at each site relative to the GPS measured location of the light source can be seen in figure 7.

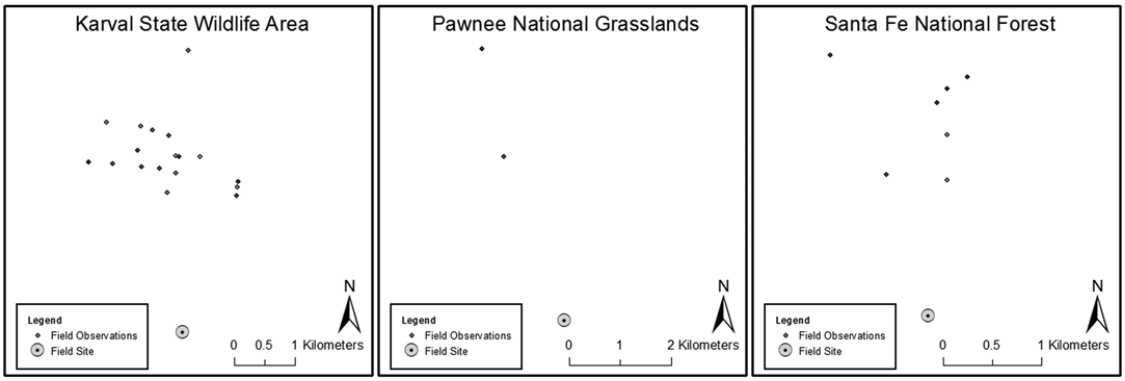

Figure 7 – Maps of GPS measured location at field sites and all the observed points at each site.

The overall mean for the distance between the measured GPS location and the observed location in the imagery was 2.90km and the median was 2.81km. For all the data points collected the mean and median bearing are the same at -0.05 degrees. The mean distance is just slightly larger, by 0.2km, than one smooth pixel and just over five times larger than one fine pixel. Additionally, the shift appears to be systematic in nature with the shift being about one smooth pixel almost directly to the North in all cases. Since the shift appears to be systematic it should be easy to correct by shifting the data by approximately one smooth pixel to the south. Applying a simple shift would be beneficial in studies merging or comparing this data with other data sets.

The means and medians grouped by satellite in table 1 show that F16 (8 data points) has a slightly lower mean at 2.49km (standard deviation of 0.72) than F18 (20 data points) at 2.88km (standard deviation of 0.9), while the medians are nearly identical. This difference is likely due to two points collected by F18 with distances of 4.582km and 5.436km from the measured GPS point. The maximum distance from the GPS for any F16 points was 3.314km. Anecdotal observations of the data by regular users suggest these slightly higher offsets can be seen in data from F16 as well. It is possible that with a larger sample size similar distances would have been seen with F16 bringing the means closer together. For F16 the mean bearing from the GPS point to the observer location is -0.05 degrees and the median is -0.03 degrees. Satellite F18 has a mean bearing of -0.06 and a median bearing of -0.07.

Looking at the data grouped by pixel resolution the smooth data (17 data points) have a higher mean and median distance from the measured GPS point than the fine (11 data points) data (table 1). The smooth data are collected by averaging a 5x5 grid of fine pixels taking the pixel resolution from 0.55km^2 to 2.7km^2. This process may account for the slight increase in the offset for the smooth data. The smooth data has a mean bearing of -0.10 degrees and a median of -0.11 degrees from the GPS point to the observed location. The fine data have a mean bearing of 0.01 degrees and a media of 0.03 degrees.

When broken out by both satellite and resolution the F16 smooth (5 data points) data has a lower mean and median of 2.59km and 2.85km, respectively, than the F18 smooth (12 data points) data. These lower distances are likely due to the reasons discussed when examining F16 vs. F18 as the two data points with higher offsets were in the smooth data. The F18 smooth has a mean of 3.13km and a median of 2.94km. The

F16 fine (3 data points) data has a lower mean at 2.32km, but a higher median at 2.58km, than the F18 fine (8 data points) data. The F18 fine data has a mean of 2.51km and a median of 2.45km.

Table 1 – The mean, standard deviation, confidence interval, first quartile, median, and third quartile of the distance and mean/median bearing between the GPS measured site locations and the observed locations in the imagery aggregated by satellite and sensor resolution.

DISTANCE	**n**	**Mean Distance (km)**	**Standard Deviation**	**95% Confidence Interval**	**First Quartile**	**Median Distance (km)**	**Third Quartile**
Overall	28	2.90	1.00	2.53 — 3.28	2.35	2.81	3.28
F16	8	2.49	0.72	1.99 — 2.99	2.25	2.72	2.90
F18	20	2.88	0.90	2.49 — 3.28	2.31	2.75	3.22
OLS	17	2.97	0.98	2.51 — 3.44	2.54	2.86	3.31
OLF	11	2.46	0.54	2.14 — 2.78	2.22	2.45	2.79
F16OLS	5	2.59	0.73	1.95 — 3.23	2.54	2.85	2.87
F18OLS	12	3.13	1.05	2.53 — 3.72	2.58	2.94	3.43
F16OLF	3	2.32	0.84	1.37 — 3.27	1.98	2.58	2.79
F18OLF	8	2.51	0.45	2.20 — 2.82	2.25	2.45	2.76

Table 2 shows the mean, standard deviation, confidence interval, first quartile, median, and third quartile of the bearing in degrees (reported between -180° and 180° where north is 0°). Measured from the measured GPS location to the observed location the F16 smooth data has a mean bearing of -0.06 degrees and a median bearing of -0.02 degrees. The mean bearing of the F18 smooth data is -0.12 degrees and the median bearing is -0.14 degrees. For the F16 fine data the mean bearing is -0.04 degrees, while the median bearing is -0.04 degrees. Finally, for the F18 fine data the mean bearing is 0.03 degrees, and the median bearing is 0.05 degrees.

Table 2 – The mean, standard deviation, confidence interval, first quartile, median, and third quartile of the bearing between the GPS measured site locations and the observed locations in the imagery aggregated by satellite and sensor resolution.

BEARING	**n**	**Mean Bearing (-180° to 180°)**	**Standard Deviation**	**95% Confidence Interval**	**First Quartile**	**Median Bearing (-180° to 180°)**	**Third Quartile**
Overall	28	-0.05	0.21	-0.12 — 0.03	-0.21	-0.05	0.08
F16	8	-0.05	0.22	-0.20 — 0.10	-0.22	-0.03	0.11
F18	20	-0.06	0.19	-0.14 — 0.02	-0.20	-0.07	0.07
OLS	17	-0.10	0.21	-0.20 — 0.00	-0.28	-0.11	0.01
OLF	11	0.01	0.15	-0.08 — 0.10	-0.10	0.03	0.10
F16OLS	5	-0.06	0.27	-0.29 — 0.18	-0.32	-0.02	0.11
F18OLS	12	-0.12	0.19	-0.23 — -0.01	-0.25	-0.14	-0.02
F16OLF	3	-0.04	0.15	-0.21 — 0.14	-0.11	-0.04	0.04
F18OLF	8	0.03	0.16	-0.08 — 0.13	-0.10	0.05	0.10

Tables 3 and 4 show the mean, standard deviation, confidence interval, first quartile, median, and third quartile of the distance in kilometers and the bearing in degrees (reported between -180° and 180°) grouped by site. There were 18 data points for the Karval State Wildlife Area, eight data points for the Santa Fe National Forest, and two data points for the Pawnee National Grasslands. Since there are only two points at the Pawnee National Grasslands site median is not reported. For each site the mean and median are very close if not identical. The Santa Fe National Forest had the lowest mean and median distance, while the Pawnee National Grasslands had the highest mean distance. If more points had been collected at the Pawnee National Grasslands site, it would likely have had a lower mean similar to the other sites. The Karval State Wildlife

Area has the most points and its mean falls between the other two sites. The mean and median bearings are very close together with a range across 0.36°. These results suggest that the distance and bearing are very similar at different geographic sites and it is expected that increased data points would bring these values even closer together. In fact none of the differences between offset distances and bearings between locations and satellites are significantly different on a statistical basis. Future research would benefit from collecting more points at the Santa Fe National Forest and Pawnee National Grasslands sites to confirm that a higher number of data points bring the means closer together across sites.

Table 3 - The mean, standard deviation, confidence interval, first quartile, median, and third quartile of the distance between the GPS measured site locations and the observed locations in the imagery aggregated by site.

DISTANCE	**n**	**Mean Distance (km)**	**Standard Deviation**	**95% Confidence Interval**	**First Quartile**	**Median Distance (km)**	**Third Quartile**
Karval State Wildlife Area	18	2.95	0.54	2.70 — 3.20	2.60	2.85	3.01
Santa Fe National Forest	8	1.97	0.53	1.60 — 2.34	1.45	2.01	2.34
Pawnee National Grasslands	2	4.37	1.50	2.29 — 6.45	N/A	N/A	N/A

Table 4 - The mean, standard deviation, confidence interval, first quartile, median, and third quartile of the bearing between the GPS measured site locations and the observed locations in the imagery aggregated by site.

BEARING	n	Mean Bearing (-180° to 180°)	Standard Deviation	95% Confidence Interval	First Quartile	Median Bearing (-180° to 180°)	Third Quartile
Karval State Wildlife Area	18	-0.06	0.20	-0.15 — 0.03	-0.18	-0.06	0.01
Santa Fe National Forest	8	0.00	0.17	-0.12 — 0.12	-0.03	0.08	0.11
Pawnee National Grasslands	2	-0.28	0.07	-0.38 — -0.18	-0.31	-0.28	-0.25

It was hypothesized that the scan angle of the sensor at the time of collection might have had an impact on both the distance and bearing of the observed location from the measured GPS location. This hypothesis was tested by plotting smooth and fine data distance and bearing against the sample, which reflects scan angle, to examine this possibility. Figure 8 shows distance vs. scan angle for the smooth data points. The R^2 is 0.01 showing no relationship between distance and scan angle for the smooth data. Figure 9 displays the distance vs. scan angle for the fine data points. The R^2 of 0.03 shows no relationship between distance and scan angle for fine data either. Figure 10 charts bearing vs. scan angle for the smooth data points. The R^2 is 0.10 which means there is no relationship between bearing and scan angle for the smooth data. Figure 11 shows bearing vs. scan angle for the fine data points. The R^2 of 0.16 again demonstrates there is no relationship between bearing and scan angle for the fine data. Overall there is no relationship between distances or bearing, from the measured GPS point, and scan angle.

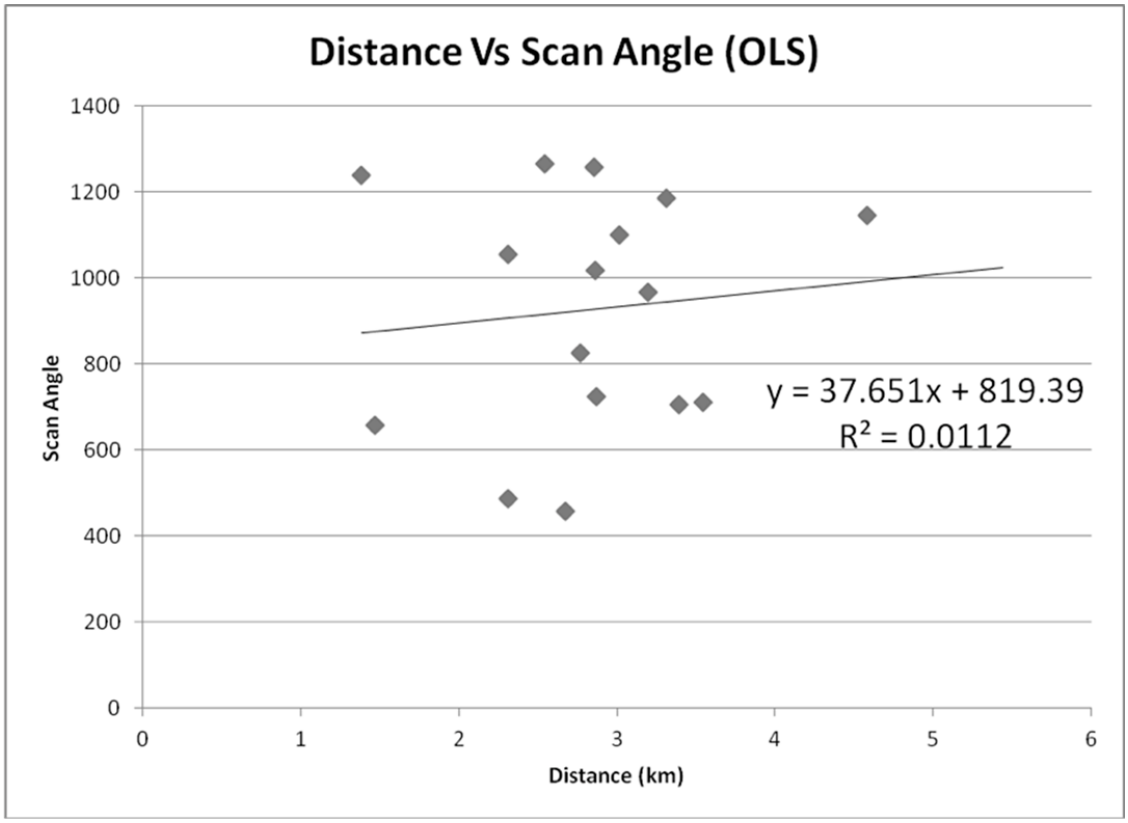

Figure 8 – Graph of distance vs scan angle for the OLS data.

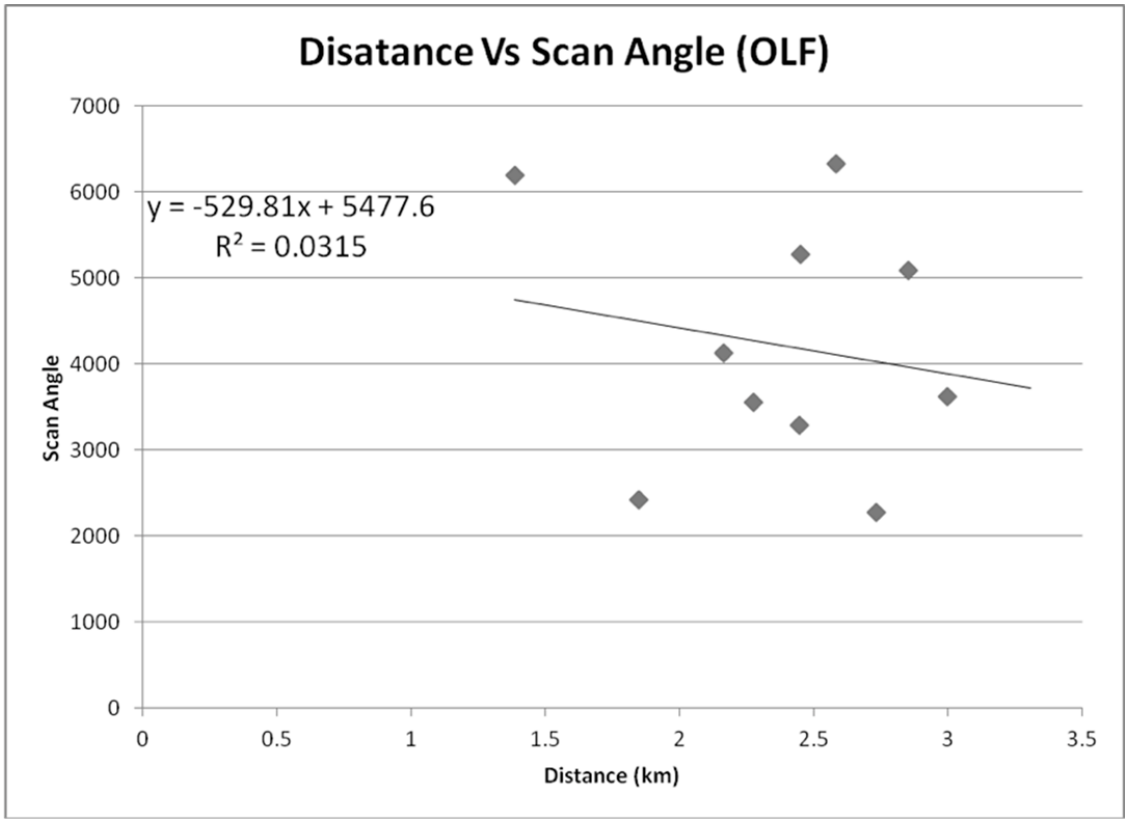

Figure 9 - Graph of distance vs scan angle for the OLF data.

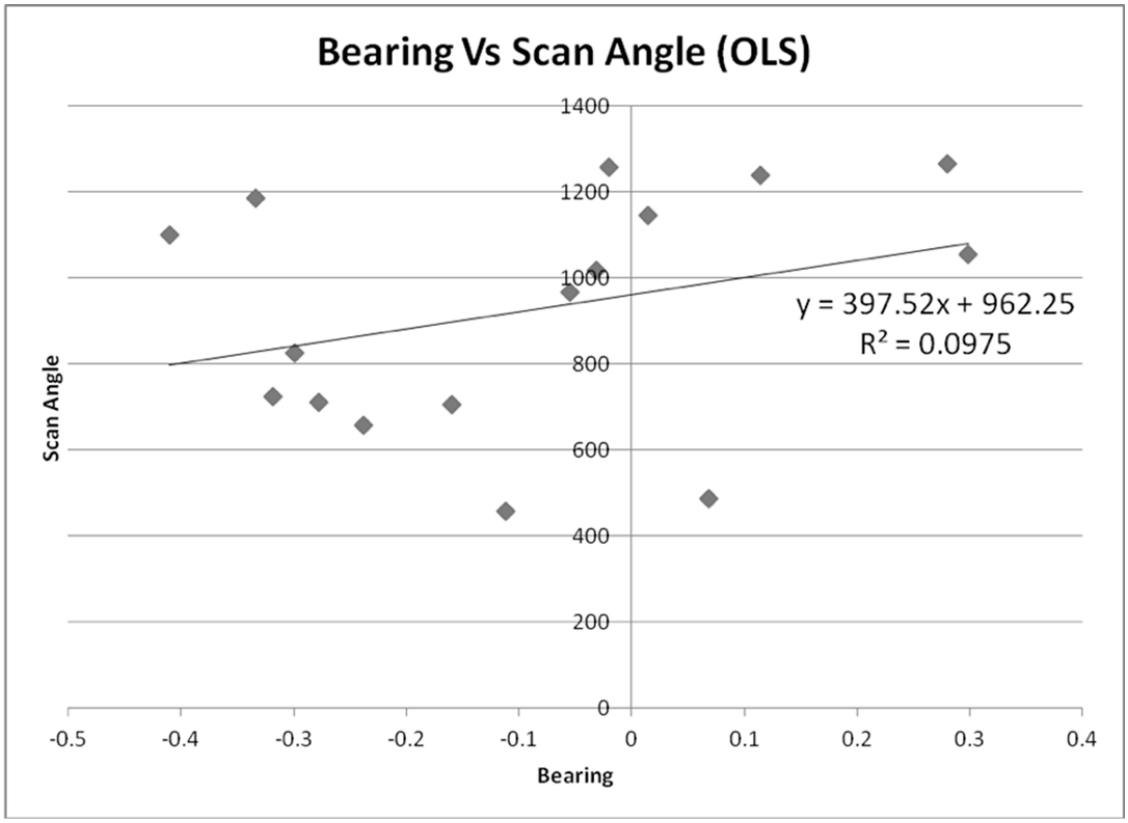

Figure 10 - Graph of bearing vs scan angle for the OLS data.

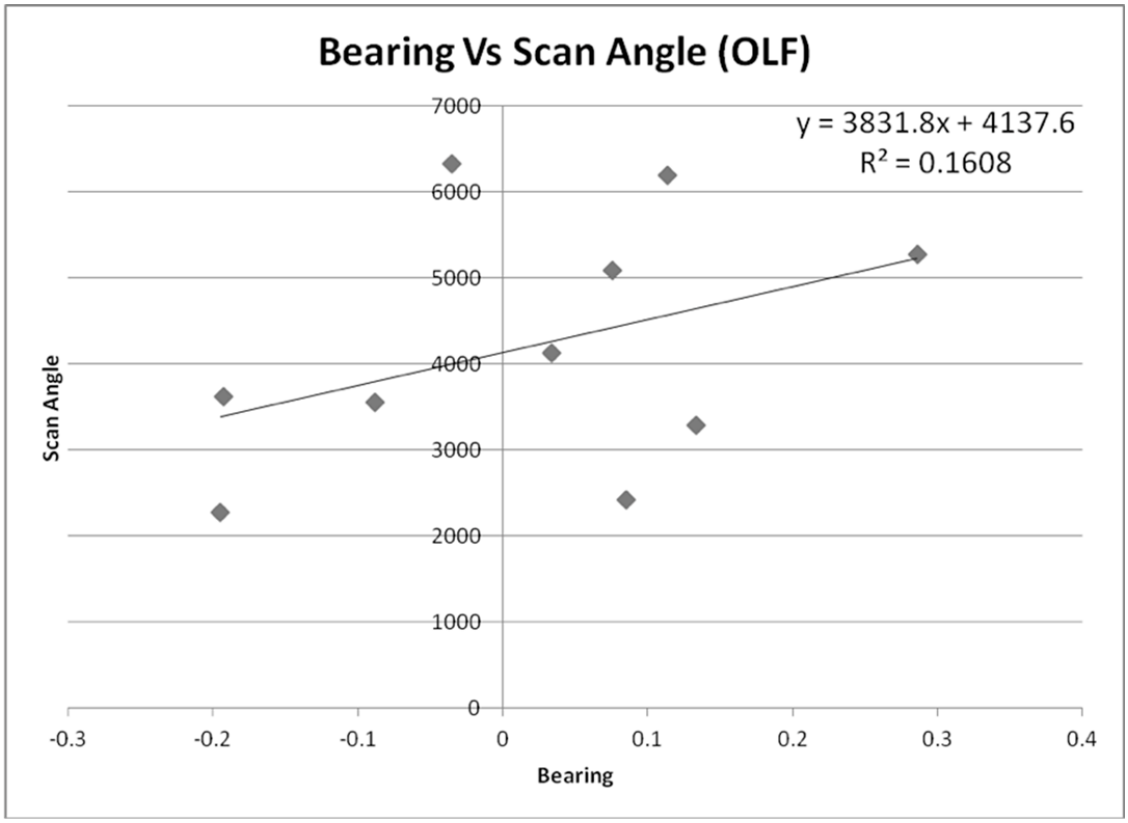

Figure 11 - Graph of bearing vs scan angle for the OLF data.

CONCLUSION

A portable lighting system capable of detection by the DMSP-OLS was designed and built. Three completely dark locations where the light could be setup were selected and GPS measurements of the locations were collected. Using the lights and these dark locations a repeatable process for measuring the location of the portable light and comparing it to the observed location in the DMSP-OLS imagery was defined. Between 18 March 2009 and 1 April 2011 the portable light system was taken to these sights on 27 separate nights. On 13 of those nights the usable data points with no cloud cover were collected. The other 14 nights had cloud cover that obscured the light or the quantity of lights used was too dim to be observed. On the 13 nights when successful data points were observed a total of 28 images were collected. It was possible to collect multiple

images in one night as there were two satellites (F16 and F18) in orbit, on some nights a satellite would observe the light twice, and on certain nights both smooth and fine data were collected.

The mean distance between the measured GPS points of where the lights were setup and the observed locations of the light in the imagery was 2.9 km (with a 95% confidence interval of 2.53-3.28 km) The median of these 28 observations was 2.81km. The mean bearing measured from the GPS point to the observed location was -0.05° (measured between -180° and 180° with a 95% confidence interval of -.12°- to -.03° - essentially due north). The median of these 28 observations was also -0.05°.This is just over a one smooth pixel shift to the north and a five fine pixel shift to the north. This shift appears to be systematic in nature and the fact that it is essentially the same for both satellites suggests the cause of the error is common to both satellites.

The data were collected at multiple sites in part to confirm either a random or systematic shift. Across the sites the bearing was in roughly the same direction ranging across 0.36°. The distances had a higher range across sites at 2.4km, however, two of the sited had far fewer images collected. The site with 18 images was in line with the overall average with a mean distance of 2.95km between the GPS measured location of the light and the observed location in the imagery. It is expected that increasing the number of collections at the other sites, which had 8 images and 2 images, would bring them more in line with the overall average. Future research should include positioning the portable lighting system described here to determine if the systematic shift identified in this study is similar around the world. The results of this study suggest that the data products should be shifted by one smooth pixel to the south to correct for the geolocation offset identified.

ACKNOWLEDGEMENTS

This research was funded in part by and NASA Earth and Space Science Fellowship and an ASPRS Rocky Mountain Region Scholarship. The authors wish to thank all the individuals at the Colorado Division of Wildlife and the National Forest Service who helped to organize access to the field sites as well as the Air Force Weather Agency for their support. Additionally, thank you to all the individuals who assisted in the various field expeditions.

REFERENCES

Baugh, K.,C. Elvidge, T. Ghosh, D. Ziskin, 2010. Development of a 2009 Stable Lights Product using DMSP-OLS data, *Proceedings of the 30th Asia-Pacific Advanced Network Meeting*, 9-13 August 2010, Hanoi, Vietnam, pp. 114-130

Cova, T. J., P. C. Sutton, D. M. Theobald. 2004. Exurban change detection in fire-prone areas with nighttime satellite imagery, *Photogrammetric Engineering and Remote Sensing*, 70(11):1249-1257

Cuartero, A., A. M. Felicisimo, M. E. Polo, A. Caro, P. G. Rodriguez 2010. Positional Accuracy Analysis of Satellite Imagery by Circular Statistics, *Photogrammetric Engineering and Remote Sensing*, 76(11): 1275-1286

Dolloff, J. and R. Settergren. 2010. An Assessment of WorldView-1 Positional Accuracy based on Fifty Contiguous Stereo Pairs of Imagery, *Photogrammetric Engineering and Remote Sensing*, 76(8):935-943

Elvidge C.D., D.M. Keith, B.T. Tuttle, K.E. Baugh, 2010. Spectral Identification of Lighting Type and Character, *Sensors*, 10(4):3961-3988

Elvidge, C. D., D. Ziskin, K. E. Baugh, B. T. Tuttle, T. Ghosh, D. W. Pack, E. H. Erwin, M. Zhizhin, 2009. A Fifteen Year Record of Global Natural Gas Flaring Derived from Satellite Data, *Energies*, 2(3):595-622

Elvidge, C.D., B. T. Tuttle, P. C. Sutton, K. E. Baugh, A. T. Howard, C. Milesi, B. Bhaduri, R. Nemani, 2007. Global distribution and density of constructed impervious surfaces, *Sensors*, 7: 1962-1979

Elvidge, C.D., C. Milesi, J. B. Dietz, B. T. Tuttle, P. C. Sutton, R. Nemani, J. E. Vogelmann, 2004(a). U.S. constructed area approaches the size of Ohio, *EOS Transactions,* American Geophysical Union, 85:233

Elvidge, C.D., J. Safran, I. L. Nelson, B. T. Tuttle, V. R. Hobson, K. E. Baugh, J. B. Dietz, E. H. Erwin, 2004(b). Area and position accuracy of DMSP nighttime lights data, *Remote Sensing and GIS Accuracy Assessment* (R. S. Lunetta and J. G. Lyon, editors), CRC Press, New York, N. Y., pp. 281-292

Elvidge, C.D., M. L. Imhoff, K. E. Baugh, V. R. Hobson, I. Nelson, J. Safran, J. B. Dietz, B. T. Tuttle, 2001(a). Nighttime lights of the world: 1994-95, ISPRS *Journal of Photogrammetry and Remote Sensing*, 56:81-99

Elvidge, C.D., I. Nelson, V. R. Hobson, J. Safran, K. E. Baugh, 2001(b). Detection of fires at night using DMSP-OLS data, *Global and Regional Vegetation Fire Monitoring from Space: Planning a Coordinated International Effort* (F. J. Ahern, J. G. Goldammer, and C. O. Justice, editors), SPB Academic Publishing bv, The Hague, The Netherlands, pp. 125-144

Elvidge, C.D., K. E. Baugh, J. Dietz, T. Bland, P. C. Sutton, H. W. Kroehl,, 1999. Radiance Calibration of DMSP-OLS Low-Light Imaging Data of Human Settlements, *Remote Sensing of Environment*, 68(1):77-88

Elvidge, C.D., K. E. Baugh, E. A. Kihn, H. W. Kroehl, E. R. Davis, 1997(a). Mapping of city lights using DMSP Operational Linescan System data, *Photogrammetric Engineering and Remote Sensing*, 63:727-734

Elvidge, C.D., K. E. Baugh, E. A. Kihn, H. W. Kroehl, E. R. Davis, C. Davis, 1997(b), Relation between satellite observed visible - near infrared emissions, population, and energy consumption, *International Journal of Remote Sensing*, 18:1373-1379

Ghosh, T., S. Anderson, R. L. Powell, P. C. Sutton, C. D. Elvidge, 2009. Estimation of Mexico's Informal Economy and Remittances Using Nighttime Imagery, *Remote Sensing*, 1(3):418-444

Ghosh, T., R. L. Powell, S. Anderson, P. C. Sutton, C. D. Elvidge, 2010. Informal Economy And Remittance Estimates of India Using Nighttime Imagery, *International Journal of Ecological Economics & Statisitics*, 17(P10):16-50

Henderson, M., E. T. Yeh, P. Gong, C. D. Elvidge, K. Baugh, 2003. Validation of urban boundaries derived from global night-time satellite imagery, *International Journal of Remote Sensing*, 24:595-609

Imhoff, M.L., W. T. Lawrence, D. C. Stutzer, C. D. Elvidge, 1997. A Technique for Using Composite DMSP/OLS 'City Lights' Satellite Data to Accurately Map Urban Areas, *Remote Sensing of Environment*, 61:361-370

Lo, C. P., 2001. Modeling the population of China using DMSP Operational Linescan System nighttime data, *Photogrammetric Engineering and Remote Sensing* 67(9):1037-1047.

Milesi, C., C. D. Elvidge, R. R. Nemani, S.W. Running, 2003. Assessing the impact of urban land development on net primary productivity in the southeastern United States, *Remote Sensing of Environment*, 86:273 – 432

O'Hara, C. G., T. Cary, K. Schuckman, 2010. Integrated Technologies for Orthophoto Accuracy Verification and Review, *Photogrammetric Engineering and Remote Sensing*, 76(10): 1097-1103

Qiao, G., W. Wang, B. Wu, C. Liu, Li R, 2010. Assessment of Geo-positioning Capability of High Resolution Satellite Imagery for Densely Populated High Buildings in Metropolitan Areas, *Photogrammetric Engineering and Remote Sensing*, 76(8):923-934

Schneider, A., M. A. Friedl, D. K. Mciver, C. E. Woodcock, 2003. Mapping urban areas by fusing multiple sources of coarse resolution remotely sensed data, *Photogrammetric Engineering and Remote Sensing*, 69(12): 1377-1386

Small, C., F. Pozzi, C. D. Elvidge, 2005. Spatial analysis of global urban extent from DMSP-OLS nighttime lights, Remote Sensing of Environment, 96:277-291

Surazakov, A. and V. Aizen, 2010. Positional Accuracy Evaluation of Declassified Hexagon KH-9 Mapping Camera Imagery, *Photogrammetric Engineering and Remote Sensing*, 76(5):603-608

Sutton P., 1997. Modeling population density with night-time satellite imagery and GIS, *Computers Environment and Urban Systems*, 21 (3/4):227–244

Sutton, P., C. Roberts, C. Elvidge, H. Meij. 1997. A comparison of nighttime satellite imagery and population density for the continental united states, *Photogrammetric Engineering and Remote Sensing,* 63(11):1303-1313

Sutton, P. C., C. Elvidge, T. Obremski. 2003. Building and evaluating models to estimate ambient population density, *Photogrammetric Engineering and Remote Sensing*, 69(5):545-553